Drastic enhancement of crystal nucleation in a molecular liquid by its liquid–liquid transition

Rei Kurita[a,1] **and Hajime Tanaka**[a,2]

[a]Department of Fundamental Engineering, Institute of Industrial Science, University of Tokyo, Tokyo 153-8505, Japan

Edited by Pablo G. Debenedetti, Princeton University, Princeton, NJ, and approved October 31, 2019 (received for review June 4, 2019)

Crystallization is one of the most familiar and fundamental phase transition phenomena. There is a possibility that crystallization may be enhanced by critical-like fluctuations associated with another nearby phase transition if the order parameter of the former is coupled to that of the latter; however, the mechanism of such order parameter coupling and its generality remain elusive due to the lack of experimental studies. Here we report experimental evidence for a nontrivial coupling between crystallization and liquid–liquid transition (LLT) for a molecular liquid, triphenyl phosphite. We find that the crystal nucleation frequency is drastically enhanced by short-time preannealing near but above the spinodal temperature of LLT. By successfully separating the thermodynamic and kinetic factors governing crystal nucleation, we show that this enhancement is induced by the lowering of the crystal–liquid interfacial energy due to the presence of critical-like order parameter fluctuations. This finding may be regarded as a fingerprint of the presence of LLT below the melting point. Thus, it may allow us not only to control the crystal nucleation frequency by LLT but also to unveil LLT hidden behind crystallization. This enhancement of nucleation frequency by critical-like fluctuations of another ordering phenomenon may be general to a variety of combinations of phase transitions. It would provide a way to control a crystal grain structure, which is a crucial control factor of mechanical and thermal properties of crystalline materials.

crystal nucleation | critical-like fluctuations | liquid–liquid transition | interface tension | order parameter

Crystallization is a nonequilibrium transformation process from a disordered liquid state to an ordered crystalline state. The resulting final crystalline structure is basically controlled by 2 kinetic factors, the nucleation frequency and the growth speed of crystals. The phenomenon of crystallization and its control are important not only in condensed matter physics but also in biology and in many industrial applications, including the phase-change memory of calcogenides, nanocrystalline materials for magnetic applications, protein crystallization, and cryopreservation. After long and intensive research, the essential physics of nucleation and growth of crystals in a macroscopic scale has been reasonably understood in the framework of the classical nucleation theory (CNT) (1–5); however, even now, there still remain many fundamental open issues such as many orders of magnitude differences in the crystal nucleation rate between experiments and numerical simulations (see, e.g., refs. 6–10).

According to CNT (1–4, 6), the crystal nucleation frequency J is given by

$$J = \frac{k_n}{\tau_t} \exp[-\Delta G^c / k_{\rm B} T], \qquad [1]$$

where k_n is a prefactor, τ_t is the characteristic time of material transport, $k_{\rm B}$ is the Boltzmann factor, and T is the temperature. Here ΔG^c is the free-energy barrier for the formation of a critical nucleus, and it is a key thermodynamic factor governing J. According to CNT, assuming the spherical shape of a nucleus, the critical nucleus size is estimated as $r_c = 2v_m\gamma/\delta\mu$, where $\delta\mu$ is the chemical potential difference between the supercooled liquid and the crystal per molecule, γ is the interfacial tension between them, and v_m is a volume per molecule. Then, ΔG^c is obtained as

$$\Delta G^c = 16\pi v_m^2 \gamma^3 / (3\delta\mu^2). \qquad [2]$$

Note that $\delta\mu$ is an increasing function of the degree of supercooling $\Delta T = T_{\rm m} - T$, where $T_{\rm m}$ is the melting point. We may assume that $\delta\mu \approx \Delta H_f (1 - T/T_{\rm m})$ near $T_{\rm m}$, where ΔH_f is the enthalpy of fusion per molecule. Note that γ is often assumed to be temperature-independent in CNT. In reality, it may depend on temperature and nucleus size (6, 8, 11). On the other hand, the kinetic factor governing J is τ_t, which is the characteristic time of material transport controlling crystallization. We note that the nucleation kinetics is controlled not by the viscosity (or rotational diffusion) but by the translational diffusion (see, e.g., refs. 12–14). We stress that the decoupling in the temperature dependence between the viscosity and the translational diffusion coefficient becomes more and more significant with an increase in ΔT, which is known as the violation of the Stokes–Einstein relation. After nucleation, a crystal grows with the growth velocity given by

$$\mathcal{V} = \frac{k_v}{\tau_t} [1 - \exp(-\delta\mu / k_{\rm B} T)], \qquad [3]$$

where k_v is a constant. It is worth mentioning that $\mathcal{V}$ is independent of γ. Unlike the nucleation frequency, experimental results of the crystal growth speed are rather well described by Eq. **3**, (15).

Significance

Contrary to our intuition, even a single-component substance may have more than 2 liquid states. The transition between them is called "liquid–liquid transition (LLT)." Recently, we have accumulated evidence for the presence of LLT. This transition may have a strong influence on crystallization, if it exists below the melting point of the crystal. Here we show that crystal nucleation rate can indeed be enhanced by many orders of magnitude near the spinodal point of LLT. This may be used not only for the control of crystalline morphology but also for searching LLT in a metastable state, which is hidden behind crystallization. Our finding also sheds light on how crystallization and other liquid-state transitions can be coupled.

Author contributions: H.T. designed research; R.K. performed research; R.K. and H.T. analyzed data; and R.K. and H.T. wrote the paper.

The authors declare no competing interest.

This article is a PNAS Direct Submission.

[1]Present address: Department of Physics, Tokyo Metropolitan University, Tokyo 192-0397, Japan.

[2]To whom correspondence may be addressed. Email: tanaka@iis.u-tokyo.ac.jp.

This article contains supporting information online at https://www.pnas.org/lookup/suppl/doi:10.1073/pnas.1909660116/-/DCSupplemental.

First published November 25, 2019.

The liquid-to-crystal transformation can be described by the change in the relevant order parameters. The most obvious important order parameter is translational order (or density). CNT assumes that a crystal nucleus has exactly the same structure as the bulk equilibrium crystal and the only difference between the nucleus and the bulk crystal is the surface energy contribution. Since the breakdown of orientational symmetry is automatically accompanied by that of translational symmetry upon crystallization, CNT completely ignores the role of the orientational ordering. Recently, however, the important role of bond orientational order has been revealed on the basis of numerical (12, 16–19) and experimental (20) studies of crystallization. More specifically, precursors with high crystal-like bond-orientational order, which are spontaneously formed as fluctuations in a supercooled liquid, reduce the liquid–crystal interfacial tension and thus promote crystal nucleation: The friendliness of the precursor structure to the crystal one controls the ease of crystallization. Although the presence of an extra order parameter other than translational order parameter is not considered in CNT, these studies have shown that, even for ordinary crystallization, a coupling between translational and orientational orderings has a drastic impact on crystal nucleation. In general, this scenario should work if there is a coupling between crystallization and another type of ordering phenomena such as phase separation (21) and liquid–liquid transition (LLT).

In a seminal paper, ten Wolde and Frenkel (22) showed that density fluctuations near a gas–liquid critical point in a supercooled state can significantly increase the crystal nucleation frequency by many orders of magnitude. More specifically, they studied, by using numerical simulations, how the presence of the gas–liquid critical point of a colloidal suspension affects crystal nucleation. In the first stage of the process, density fluctuations grow without accompanying translational ordering. Then, in the next stage, crystal ordering proceeds selectively in high-density regions. They showed that this 2-step kinetic pathway drastically reduces the liquid–crystal interfacial tension, because of preferential wetting of higher-density regions to the crystal, indicating that the presence of critical density fluctuations drastically enhances the nucleation frequency of colloid crystals (22). Then this scenario was supported theoretically (23–25). Here we note that the underlying physics is the same between the impact of density fluctuations linked to a gas–liquid criticality and that of the above-mentioned bond-orientational order fluctuations in a supercooled liquid.

This problem was also studied experimentally in protein solutions, and the enhancement of the nucleation rate was indeed observed near the binodal line (26, 27); however, the maximum of the nucleation rate is located several degrees above the spinodal temperature T_{SD}, but not at T_{SD}. Considering that the above-described thermodynamic argument at the mean field level predicts the nucleation frequency to be maximized at T_{SD}, the deviation of the maximum from T_{SD} has cast some doubt on the origin of the crystal nucleation enhancement. For example, this discrepancy might be explained by the slowing down of the kinetics, or the increase in τ_t: An increase in the viscosity of dense liquid droplets may decrease the nucleation rate (26, 27). Possible glassiness of the intermediate metastable phase was also suggested (28). In addition, the role of the temperature dependence of γ may not be ruled out. At this moment, thus, there is no firm consensus on the origin of the discrepancy (see, e.g., ref. 18 for a review). For elucidating the very origin of the enhancement, thus, it is crucial to disentangle the thermodynamic ($\delta\mu$ and γ) and kinetic factors (τ_t).

The key to crystal nucleation enhancement due to criticality is the reduction of the crystal–liquid interfacial tension γ due to fluctuations of an extra order parameter in the liquid state. For this to happen, the order parameter with criticality must be coupled to crystalline order parameter(s). Then the next questions are how strong the coupling is and how large the order parameter fluctuations are. Criticality is crucial for the realization of large amplitude and long correlation length of the fluctuations. This consideration leads to a conclusion that this physical mechanism of crystal nucleation enhancement should be valid universally to any phase ordering, provided that it is located below the melting point and fluctuations of its order parameter efficiently reduce the crystal–liquid interfacial tension γ.

Here we take, as such an example of phase-ordering phenomena, LLT that is a phase transition between multiple liquid states in a single-component liquid (2). Recently, there are many pieces of experimental and theoretical evidence for the existence of LLT in single-component systems (2, 29–35). Polyamorphic transitions were suggested for water (34). Furthermore, the existence of LLT has also been suggested for important atomic elements, such as Si, C, S, and Se (29, 31, 33). However, for many of these liquids, including water, LLT is expected to occur in their metastable supercooled liquid states, often far below T_m (29, 33, 34); that is, LLT is hidden behind crystallization. This makes experimental investigations of the phenomena quite challenging. Thus, the influence of the presence of LLT on crystallization is also important for studying LLT itself.

It might be a bit counterintuitive to accept 2 liquid states for a pure substance. We argued that LLT is controlled by a new order parameter S, which is the fraction of locally favored structures (12, 36). According to this 2-order-parameter model, LLT can be viewed as a gas–liquid transition of this order parameter S (i.e., the 2 liquids are S-rich and S-poor liquids in our model), whereas the normal gas–liquid transition is a transition of the density order parameter. The density is conserved in a system, and thus its change at a certain position must be accompanied by a change in nearby density. On the other hand, locally favored structures can be created and annihilated rather independently, and thus the order parameter S is a nonconserved order parameter (37).

Some time ago, we found experimental evidence for LLT in a molecular liquid, triphenyl phosphite (TPP) (12) (see Fig. 1 for the key temperatures of TPP). We identified 2 types of transformation from liquid I to liquid II, nucleation growth (NG) and spinodal decomposition (SD) type. For TPP, NG-type

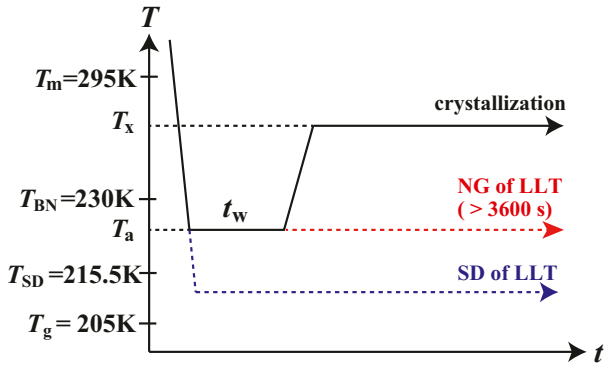

Fig. 1. Key temperatures of TPP and a special temperature protocol used in our experiments. The melting point T_m of TPP is located at 295 K. LLT takes place below the binodal temperature $T_{BN} = 230$ K. The transformation kinetics of LLT from liquid I to liquid II can be classified into 2 types: NG and SD type. NG-type transformation takes place between $T_{BN} = 230$ K and the spinodal temperature $T_{SD} = 215.5$ K, whereas SD-type one takes place below $T_{SD} = 215.5$ K. Since T_{BN}(=230 K) is located below T_m (=295 K), LLT always takes place in a metastable supercooled state. We anneal TPP for t_w at T_a in order to create S fluctuations near but above T_{SD}. Then we heat it to T_x for crystallization under influence of S fluctuations. The glass transition temperature T_g is located at 205 K slightly below T_{SD}.

transformation takes place between the spinodal temperature $T_{SD} = 215.5$ K and the binodal temperature $T_{BN} = 230$ K, while the transformation is SD-type below $T_{SD} = 215.5$ K (38, 39). Since the melting point T_m is located at 295 K, LLT always takes place in a metastable supercooled state. We found that the transition between NG-type and SD-type LLT is rather sharp, indicative of the mean field nature of the transition. This is suggestive of enhancement of critical-like fluctuations of S near T_{SD}. This is because, when approaching T_{SD} from above, the metastable state approaches an unstable state. Such enhancement is known to be more significant for a system with stronger mean field nature. The mean field nature is stronger for a system with longer bare correlation length. This is known as the Ginzburg criterion (3). In ordinary gas–liquid phase transition, for example, the bare correlation length is roughly given by the size of a molecule. On the other hand, for liquid–liquid transition, the size of locally favored structures, which are made of several molecules, is larger than the size of a single molecule. For TPP, for example, we estimated the size to be about 3 nm (40). This longer bare correlation length should lead to stronger mean field nature, or stronger enhancement of the order parameter (S) fluctuations toward T_{SD}. Indeed, we found experimental indications for the presence of critical-like order parameter fluctuations near the spinodal temperature (12, 36), including spatial confinement effects on LLT (41) and wetting effects on LLT (42). Furthermore, the longer characteristic length should lead to the longer lifetime of S fluctuations, which is proportional to the cube of the correlation length. This slow relaxation allows us to use a special protocol we use in our experiments (see below). In this article, we study the impact of S fluctuations near but above T_{SD} on crystal nucleation in TPP.

One might think that we may study this problem simply by measuring the crystal nucleation rate as a function of the crystallization temperature T_x. But we cannot take this strategy: Since the nucleation barrier of the liquid II phase rapidly decreases while approaching T_{SD} (38), NG-type LLT takes place before crystallization occurs, below 225 K (or near T_{SD}). This prevents us from studying the crystallization behavior in this temperature region with the ordinary temperature protocol. Thus, we design a special experimental protocol, as shown in Fig. 1 (see *SI Appendix*, section 1 for the details), in which the crystal nucleation rate is measured at a fixed T_x above T_{BN}, where LLT never takes place, after a short-time annealing of the melt at a temperature T_a over t_w near but above T_{SD}. During annealing at T_a, S fluctuations may grow near T_{SD} before NG-type LLT takes place. Then, after heating to T_x, if the S fluctuations remain until crystal nucleation, they might help the nucleation by reducing γ. This is our expectation based on our previous study (19), in which only γ is affected by order parameter fluctuations whereas τ_t and $\delta\mu$ are not so much. This protocol relies on a specific relationship between the growth and decay time of S fluctuations, the incubation time for crystal nucleation, the kinetics of NG-type LLT, and the characteristic time of the temperature change (see below and *SI Appendix*, section 1). It allows us not only to separate the activation energy ΔG^c of crystal nucleation from the kinetic one τ_t (Eq. **1**) but also to separate the effect of γ from that of $\delta\mu$ (Eq. **2**). Note that, in this temperature protocol, the dependencies of τ_t and $\delta\mu$ on S fluctuations are negligible for different annealing conditions (see below). So, if there is no LLT, or in the absence of the effect of S fluctuations, then γ should also be the same, and thus the crystallization behavior should not depend on T_a. We indeed confirmed this experimentally for 4 molecular liquids without LLT (see below).

First, we discuss the growth of S fluctuations at T_a and their fate after rapid heating to the crystallization temperature T_x ($> T_a$). Fig. 2 shows the dependence of the crystal nucleation rate J at $T_x = 235$ K on the annealing time t_w for $T_a = 216$ K (circles), 218 K (squares), and 220 K (triangles) (*SI Appendix*, section 2). There we can see the increase of J with an increase in t_w for the 3 T_as, and the amount of the increase is larger near T_{SD}. We stress that J should not depend on t_w if the liquid already reaches its equilibrium state with little S fluctuation at T_x just after being heated to this T_x. We also note that, above but near T_{SD}, the nucleation of liquid II droplets occurs only after a rather long induction time (>900 s), and our annealing time t_w is much shorter than this incubation time. In other words, liquid II nuclei rarely exceed the critical nucleus size, in this protocol. Thus, there can be only fluctuations of the order parameter S as long as $t_w < 900$ s. Thus, the above result clearly indicates that 1) thermal fluctuations of S grow by annealing near T_{SD} and are more enhanced when T_a is closer to but above the spinodal line T_{SD}, 2) they remain for a reasonably long time (at least for ~ 100 s [*SI Appendix*, section 2 and Fig. S1]) after being heated from T_a to T_x until crystal nuclei are formed at T_x, and 3) their presence assists the crystal nucleation. This enhancement of S fluctuations near T_{SD} may be due to the mean field-like nature of LLT.

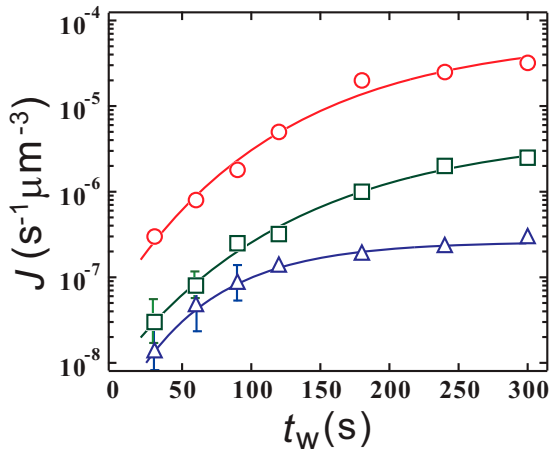

Fig. 2. The crystal nucleation rate J at T_x as a function of the annealing time t_w for $T_a = 216$ K (circles), 218 K (squares), and 220 K (triangles). For $t_w > 300$ s, J almost becomes constant, meaning that S fluctuations are quasi-equilibrated at T_a. We note that an incubation time for NG-type LLT at T_a is much longer than 300 s. Thus, the fact that the crystal nucleation rate increases when T_a is closer to T_{SD} indicates that S fluctuations are more enhanced near T_{SD} (see also the main text and *Methods*). The solid lines are fits by $J = J_S \exp[-b \exp(-t_w/\tau_S)]$, where J_S, b, and τ_S are the fitting parameters (see the main text). To reduce the statistical errors, we took an average over 10 independent experiments for each T_a. The error bars are shown in the plot only when they exceed the size of the symbols.

We also find that the dependence of J on t_w can be well described as

$$J(t_w) = J_S \exp[-b \exp(-t_w/\tau_S)], \quad [4]$$

where J_S is the final crystal nucleation rate after the establishment of quasi-equilibrium S fluctuations, which we denote S^{eq}, for long enough t_w at T_a, and thus it should be given by

$$J_S = \frac{k_n}{\tau_t} \exp[-\Delta G^c(S^{eq})/k_B T], \quad [5]$$

where $\Delta G^c(S^{eq})$ is the free-energy barrier for a liquid with fully developed S fluctuations, S^{eq}, at T_a. On the other hand, at $t_w = 0$, there are no S fluctuations, and the free-energy barrier should be given by $\Delta G^c(0)$, where 0 means the absence of S fluctuations. Thus, we obtain

$$b = [\Delta G^c(0) - \Delta G^c(S^{eq})]/k_B T = \delta\Delta G^c/k_B T. \quad \textbf{[6]}$$

Thus, b has a clear physical meaning of the thermal energy-scaled free-energy barrier difference between a liquid without and with S fluctuations. The τ_S is then the characteristic time of the growth of S fluctuations. In this way, Eq. **4** has a clear physical meaning.

From the fitting, τ_S is estimated to be 146 s at 216 K, 128 s at 218 K, and 82 s at 220 K, and, thus, much longer than the structural (density order parameter) relaxation time [$\sim 10^{-4}$ s at 216 K measured by dielectric spectroscopy (43)]. This result indicates that 1) it takes a longer time for S fluctuations to grow near T_{SD} and 2) once they are formed, they have a rather long lifetime. These 2 facts allow us to equilibrate S fluctuations at T_a and keep it at T_x with little decay even after heating from T_a to T_x until crystals are nucleated. We note that it is difficult to directly access S fluctuations experimentally. The origin of such slow growth and relaxation of S fluctuations is an important problem, but we leave it for future research.

Now we show how the S fluctuations formed at T_a and still remaining at T_x affect crystal nucleation. Using the above-mentioned protocol, we first annealed TPP at $T_a = 220$ K (Fig. 3*A*), 217 K (Fig. 3*B*), and 150 K (Fig. 3*C*) for the annealing time $t_w = 300$ s, and then heated it with a rate of 100 K/min to the target temperature $T_x = 235$ K, where crystallization takes place. Fig. 3 *A*–*C* shows images of crystalline spherulites observed with polarizing microscopy after waiting for 20 min at T_x. We can clearly see that the number of crystal nuclei is very different between the 3 cases (Fig. 3 *A*–*C*), despite the fact that all crystallization processes take place at the same temperature T_x and thus $\delta\mu$ and τ_t should be the same between them. We note that the cases in Fig. 3 *A* and *C* are far from T_{SD}, whereas the case in Fig. 3*B* is near T_{SD}.

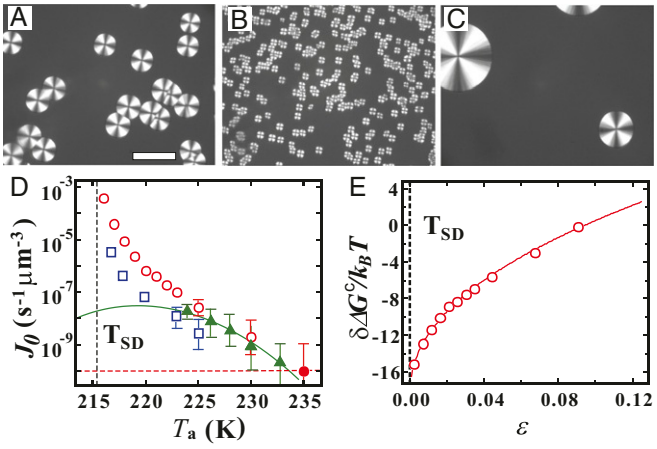

Fig. 3. Enhancement of the crystal nucleation frequency J_0 near the spinodal temperature of LLT, T_{SD}. (*A*–*C*) Images show crystals observed with polarizing microscopy in TPP samples, which were first quenched to (*A*) $T_a = 220$ K, (*B*) 217 K, and (*C*) 150 K and annealed there for 5 min, then heated to $T_x = 235$ K with a rate of 100 K/min and annealed for 20 min. We stress that the crystallization always takes place at $T_x = 235$ K. (Scale bar: *A*, 20 μm; also applies to *B* and *C*.) (*D*) The crystal nucleation rate J_0 at $T_x = 235$ K (circles) and 240 K (squares) as a function of T_a for a sample with *S* fluctuations, which is annealed at T_a for 5 min. The J_0 for the ordinary crystallization protocol is also shown by green triangles, together with the CNT prediction (green solid curve) (*SI Appendix*, section 3 and Fig. S3). This J_0 without *S* fluctuations obeys the CNT prediction, as expected. The vertical black dashed line indicates the location of T_{SD}. For both T_xs, J_0 for crystallization of a sample with *S* fluctuations increases very steeply when $T_a \to T_{SD}$. The filled red circle corresponds to J_0 for a sample directly quenched to 235 K from melt; that is, it corresponds to J_0 in absence of *S* fluctuations at $T_x = 235$ K. The horizontal red dashed line is the value of J_0 expected in the absence of LLT. For $T_a \geq 225$ K, the number of crystal nuclei becomes very small, leading to a larger statistical error. The data are the crystal nucleation rate averaged over 10 times. The error bars are shown in the plot only when they exceed the size of the symbols (*SI Appendix*, section 2) (*E*) The difference $\delta\Delta G^c$ between ΔG^c at 235 K and that at T_a as a function of $\epsilon = (T_a - T_{SD})/T_{SD}$. The solid curve is a fit by $G_0 + G_1\epsilon^\nu$ with $\nu = 0.56$ (see text).

Next, we estimate the crystal nucleation rate J_0 as a function of T_a, where J_0 is the value of J for the equilibrated state after long enough t_w (for the method to estimate J, see *SI Appendix*, section 2 and Fig. S1), for $T_x = 240$ K as a function of T_a. The enhancement of J_0 by many orders of magnitude when $T_a \to T_{SD}$ is observed for both T_xs. We stress that this increase far exceeds the maximum nucleation frequency ($\sim 10^{-8} s^{-1}\cdot\mu m^{-3}$) expected for the ordinary quench protocol (see the green solid line in Fig. 3*D*). The filled red circle in Fig. 3*D* corresponds to the nucleation rate for a liquid which is quenched directly to 235 K from melt; that is, it corresponds to J_0 in the absence of S fluctuations at $T_x = 235$ K. As will be shown below, if there is no LLT, the crystal nucleation rate is not affected by annealing, contrary to the case of TPP.

The crucial feature is the positive curvature of the temperature dependence of the crystal nucleation frequency J. This can never be explained by the ordinary classical nucleation frequency scenario, which predicts the negative curvature due to the steep decrease toward both T_m and T_g (*SI Appendix*, section 3 and Fig. S3). The only possible explanation may be crystallization of 2 polymorphs with different melting points. Although there is a systematic deviation, we can somehow fit the data with CNT assuming the 2 types of polymorphs (*SI Appendix*, section 3 and Fig. S4). However, this scenario is unlikely by the single melting behavior of only one type of crystal.

We also calculate $\delta\Delta G^c$ at $T_x = 235$ K, which is the difference in ΔG^c between the liquid without S fluctuations and the one with S fluctuations formed at T_a (Eq. **6**). Fig. 3*E* plots $\delta\Delta G^c$ as a function of the reduced temperature ϵ ($= [T_a - T_{SD}]/T_{SD}$). We find that the free-energy barrier decreases by 16 $k_B T$ toward $\epsilon = 0$. This is a comparable reduction reported by ten Wolde and Frenkel (22) for colloidal suspensions near a gas–liquid critical point. We can express $\delta\Delta G^c$ as $G_0 + G_1\epsilon^\nu$, where $G_0/k_B T = -17.9$, $G_1/k_B T = 58.3$, and $\nu = 0.56 \pm 0.10$ when $T_a > T_{SD}$, but the physical meaning of the value of the exponent ν is not clear at this moment.

Here we discuss the physical origin of the drastic enhancement of the crystal nucleation rate by our protocol. The crucial point is that the enhancement of *S* fluctuations may influence τ_t and $\delta\mu$, but the effects should be minor. For example, since τ_t contributes to the nucleation frequency as a prefactor (Eq. **1**), its small change can never lead to many orders of magnitude change in the crystal nucleation frequency. We also note that our measurements of dielectric spectroscopy show that the influence of S fluctuations on the structural relaxation time is very minor if it even exists (43). Furthermore, the enthalpy change of liquid detected by differential scanning calorimetry (DSC) measurements is also negligibly small (*SI Appendix*, section 4 and Fig. S5), indicating that the influence of S fluctuations on $\delta\mu$ should also be minor. Thus, we may assume that $\delta\mu$ depends only on T_x. This is consistent with the fact that the growth velocity $\mathcal{V}$ is independent of T_a (note that $\mathcal{V}$ depends only on $\delta\mu$ [Eq. **3**]). Thus, we may conclude that any dependence of the crystal nucleation rate, or, more specifically, $\delta\Delta G^c$, on T_a should originate mainly from the influence of S fluctuations formed at T_a on γ.

To confirm the crucial role of LLT in the observed drastic enhancement of the crystal nucleation rate by annealing near the spinodal temperature T_{SD}, here we study the effect of annealing on the rate of crystal nucleation in ordinary liquids without LLT.

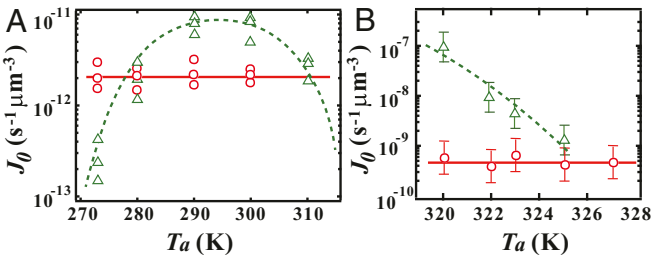

Fig. 4. Effects of annealing on the crystal nucleation rate for ordinary liquids without LLT. (*A*) The rate of crystal nucleation in D-sorbitol. The triangles correspond to J_0 when the sample is crystallized at an annealing temperature T_a. The dashed curve is the CNT fitting of the data, which are consistent with the results in ref. 44. On the other hand, the circle symbols represent the nucleation rates for a protocol in which a sample is annealed at T_a for 1 h and then heated and crystallized at $T_x = 310$ K. (*B*) The rate of crystal nucleation in PCL. The dashed curve is a guide to eye. The triangles correspond to J_0 when the sample is crystallized at T_a. The circle symbols correspond to J_0 at $T_x = 327$ K after the sample is annealed at T_a for 10 min. In both systems, the crystal nucleation rate is not affected by the annealing at temperatures below T_m.

Fig. 4*A* shows the protocol dependence of J_0 for D-sorbitol. The triangle corresponds to J_0 when the liquid D-sorbitol is annealed and crystallized at T_a. The dashed line in Fig. 4*A* is the CNT fitting of the data, which are consistent with the results reported in ref. 44. On the other hand, the circle symbols shown in Fig. 4*A* correspond to J_0 at a fixed temperature $T_x = 310$ K after the liquid is annealed at T_a for 1 h. These results clearly indicate that the nucleation rate of D-sorbitol is not affected by the annealing treatment at all. We also obtain the same conclusion for poly(ϵ-caprolactone) (PCL) (Fig. 4*B*), triphenyl phosphine (TPPN), and polyethylene glycol (PEG) (*SI Appendix*, section 5 and Fig. S6). Here it is worth noting that TPPN is a glass-forming material, which has a molecular structure similar to TPP. Thus, we may conclude that, for ordinary liquids that do not have LLT, there is no effect of such annealing on the crystal nucleation rate. Contrary to these ordinary liquids, for TPP, the nucleation rate is drastically enhanced by nearly 7 orders of magnitude with a decrease of T_a from 235 K to 215 K. This strongly indicates that the presence of LLT and the resulting enhancement of S fluctuations toward T_{SD} are responsible for such a drastic increase in the nucleation rate of crystals toward T_{SD}.

One might think that the enhancement of crystal nucleation for TPP can be due to formation of invisible crystal nuclei during annealing at T_a. But this scenario is unlikely because of the following reasons: 1) The size of nuclei should be smaller than the critical nucleus size at T_a. This is because, otherwise, we should see their continuous growth, but this was never observed before the formation of liquid II nuclei below 223 K (38). Then, on noting that the critical nucleus size should be larger at 235 K than around 215 K, this scenario cannot explain the observed enhancement. 2) For this scenario, the crystal nucleation rate J should be constant with t_w, but this is clearly inconsistent with the results shown in Fig. 1. Furthermore, the incubation time for crystallization at T_x shown in *SI Appendix*, section 2 and Fig. S1 should not be observed, and instead their immediate growth from $t_w = 0$ should be observed. 3) This scenario cannot explain a much higher nucleation rate at T_x after annealing at T_a than the rate predicted by CNT (green solid curve in Fig. 3*D*). 4) We compare J_0 between at $T_x = 240$ K and 235 K (Fig. 3*D*). We can see that J_0 decreases at higher T_x. If invisible yet large crystal nuclei are already formed during annealing at T_a, J_0 should be larger for higher temperature, since a higher growth rate at 240 K (~0.2 μm) than at 235 K (~0.1 μm) (38) (*SI Appendix*, section 2 and Fig. S2). This clearly contradicts our observation. In our scenario, we can naturally explain the lower crystal nucleation rate at higher T_x as a consequence of weaker S fluctuations there. 5) As shown in *SI Appendix*, section 4 and Fig. S5*A*, peak L in the DSC curve continuously shifts to lower temperature. If we suppose that preexisting nuclei are formed in the annealing process, we expect that crystal growth should start at the same temperature for different annealing periods and thus the DSC peak position should be the same. This contradicts our observation. 6) We also note that, if such a scenario is relevant, we should see similar behaviors in D-sorbitol, PCL, TPPN, and PEG, but we do not see any such indications, as shown in Fig. 4 and *SI Appendix*, section 5 and Fig. S6. From considerations 1 through 6, we conclude that the steep increase of J_0 toward T_{SD} is due to the enhancement of S fluctuations.

Next we study the spatial correlation between crystal nucleation sites and S fluctuations to check the coupling between the order parameters of crystallization and LLT, including its sign. To do so, we anneal TPP below T_{SD} to enhance S fluctuations by SD-type LLT, since S fluctuations cannot be directly observed above T_{SD} with optical microscopy but can be observed below T_{SD} (38). This, although not a direct proof, reveals the nature of the coupling between the order parameter of LLT (S) and that of crystallization. We show, in Fig. 5*A*, a phase-contrast microscopy image of SD-type LLT observed after annealing at 214 K ($< T_{SD}$) for $t_w = 120$ min, where dark regions correspond to high-S regions. Then, we heat the sample to $T_x = 235$ K with a rate of 20 K/min. Fig. 5*B* shows an optical microscopy image of crystal nuclei observed after annealing for 5 min at

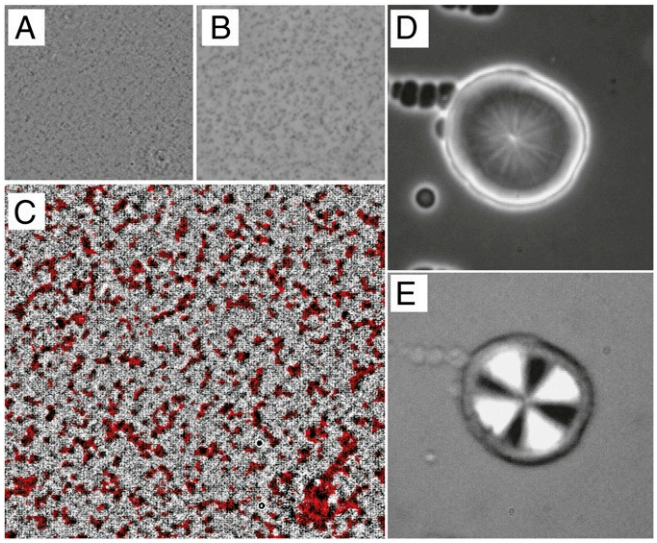

Fig. 5. Coupling between crystallization and *S* fluctuations. (*A*) Spatial fluctuations of *S* observed with phase-contrast microscopy in a sample quenched to 214 K (below T_{SD}) after annealing there for 120 min. The darker regions correspond to higher *S* regions. (*B*) Crystal nuclei (dark droplets) observed with phase-contrast microscopy in the same area as panel *A*, after heating the sample to 235 K with a rate of 20 K/min and annealing there for 5 min. (*C*) Superposition of images from *A* (gray) and *B* (red). We can see a clear spatial correlation between high-*S* regions (black) and crystal nuclei (red). (*D*) A crystal spherulite that is wet by liquid II. First the crystal was formed at 235 K, and then the sample was quenched to 220 K to initiate NG-type LLT. The image is taken 80 min after the quench. We can see that the wetting layer of liquid II is preferentially formed on the surface of the spherulite in the middle of the image. Dark small droplets of liquid II are also nucleated in bulk. (*E*) Polarizing microscopy observation of the same sample as in *D*. We can see the nonbirefringent wetting layer around the crystal spherulite with Maltese cross. The size of all images is 120 × 120 μm^2.

235 K in exactly the same region as Fig. 5*A*. To see the spatial correlation between S fluctuations and crystal nuclei, we superimpose the 2 images, S fluctuations (Fig. 5*A*) (appeared black) and crystal nuclei (Fig. 5*B*) (appeared red), in Fig. 5*C*. We can clearly see that crystal nucleation preferentially occurs in higher-S regions with darker contrast, suggesting 1) the survival of S fluctuations after heating to T_{x} and 2) lower γ in higher S regions. To be more quantitative, we estimate the probability of crystal nuclei being formed in high-S regions and find that about 93% of crystal nuclei are formed in high-S dark regions.

To further confirm this conclusion that the crystal–liquid interfacial free energy is a decreasing function of S, we also observe how LLT proceeds under an influence of a preexisting crystal. First, we prepare a crystalline spherulite by annealing TPP at a temperature above $T_{BN} = 230$ K but below $T_{\mathrm{m}} = 295$ K. Note that, under this condition, only crystallization takes place without accompanying LLT. Then we quench the system below T_{BN} to initiate NG-type LLT. We find that liquid II is preferentially nucleated on the surface of the preexisting crystal to form the wetting layer, as shown in Fig. 5 *D* and *E*. This unambiguously indicates that liquid II is more wettable for crystals than liquid I, or the crystal–liquid interfacial tension γ is a decreasing function of S (see also ref. 42). We also show other supporting evidence for the reduction of the crystal nucleation barrier by S fluctuations from DSC measurements in *SI Appendix*, section 4 and Fig. S5.

To summarize, we find the enhancement of crystal nucleation by order parameter fluctuations associated with LLT. This is clear experimental evidence that the crystal nucleation is enhanced thermodynamically near the spinodal temperature of LLT. Our study suggests the universality of the scenario proposed by ten Wolde and Frenkel (22) in relation to various types of phase transitions such as phase demixing and liquid–liquid transition. This scenario is originally proposed for phase demixing or gas–liquid transition, where the order parameter is conserved. On the other hand, the order parameter of LLT can be changed locally, or it is of nonconserved nature (12). Thus, our finding indicates that the scenario does not depend upon whether the order parameter is conserved or not, and the only crucial factor is the presence of its coupling to the crystal order parameter and the resulting reduction of the crystal–liquid interfacial tension. With the help of critical-like fluctuations, we may attain a large nucleation frequency far beyond its maximum in the ordinary quench protocol, providing a way to decrease the crystal grain size and its variance that are important factors controlling the physical properties of crystalline materials (45, 46).

This phenomenon may also be used to reveal any phase transition that is located in a supercooled state metastable against crystallization and thus hidden behind crystallization. For example, there are many candidates of LLTs, which are expected to occur far below T_{m} but hidden by crystallization: They include water, Si, Ge, and metallic liquids (29, 33, 34, 47). Our finding provides an experimental method to detect order parameter fluctuations associated with a hidden LLT in such systems by using crystallization behavior as a probe. The enhancement of the crystal nucleation frequency as a function of the preannealing temperature T_{a} at a constant crystallization temperature T_{x} can be used as a fingerprint for the presence of a hidden phase transition. We also reveal the difference in crystallization dynamics between liquid I and liquid II (*SI Appendix*, section 4 and Fig. S5). This is related to another interesting subject of research, that is, a link between crystallization behavior and LLT (see, e.g., refs. 48 and 49). For example, our study may shed light on LLT in water: For example, our study may provide insight into a recent interest in how the kinetic pathway of ordering is affected by an interplay between crystallization and LLT in a metastable supercooled water (35). Finally, we note that the physical scenario is not limited to crystallization, but may be universal to nucleation of an ordered phase under the influence of critical fluctuations associated with another phase ordering.

Methods

The sample used is TPP purchased from Aldrich Chemical Co., Inc., and used after extracting only a crystallizable part and filtering it to remove impurities that may act as nucleators for crystallization. We observed the liquid–liquid transformation process with phase-contrast and polarizing microscopy. For these observations, a sample was sandwiched between 2 cover glasses, and its thickness was controlled to be 10 μm by using monodisperse glass beads as spacers (see *SI Appendix*, section 2 for effects of the sample thickness on crystal nucleation). We confirmed that this level of spatial confinement does not affect the behaviors significantly (41). The temperature was controlled within ±0.1 K by a computer-controlled hot stage (Linkam LK-600PH) with a cooling unit (Linkam L-600A). We note that, in our phase-contrast microscopy observation, a region having a higher refractive index (or the higher density) appears with darker contrast. We also used D-sorbitol, PCL (molecular weight: 60,000), TPPN, and PEG (molecular weight: 6,000) purchased from Aldrich Chemical Co., Inc., to clarify whether the annealing at low temperatures affects crystallization for systems without LLT or not. We measured the nucleation rate of the so-called polymorph E of D-sorbitol ($T_{\mathrm{m}} = 353$ K) (44). In *SI Appendix*, section 4 and Fig. S5, we report results of our heat experiments. In the experiments, we measured the heat flux during the transformation with a differential scanning calorimeter (DSC-822e; Mettler Toledo).

ACKNOWLEDGMENTS. H.T. acknowledges support from Grants-in-Aid for Scientific Research (S) and (A) (Grants JP21224011 and JP18H03675, respectively), and Specially Promoted Research (Grant JP25000002) from the Japan Society of the Promotion of Science. R.K. acknowledges support from a Grant-in-Aid for Scientific Research (B) (Grant JP17H02945).

1. K. Binder, Theory of first-order phase transitions. *Rep. Prog. Phys.* **50**, 783–859 (1987).
2. P. G. Debenedetti, *Metastable Liquids* (Princeton University Press, Princeton, NJ, 1997).
3. A. Onuki, *Phase Transition Dynamics* (Cambridge University Press, Cambridge, United Kingdom, 2002).
4. D. Turnbull, Under what conditions can a glass be formed?*Contemp. Phys.* **10**, 473–488 (1969).
5. A. Statt, P. Virnau, K. Binder, Finite-size effects on liquid-solid phase coexistence and the estimation of crystal nucleation barriers. *Phys. Rev. Lett.* **114**, 026101 (2015).
6. K. Kelton, A. L. Greer, *Nucleation in Condensed Matter: Applications in Materials and Biology* (Elsevier, 2010), vol. 15.
7. G. F. Neilson, M. C. Weinberg, A test of classical nucleation theory: Crystal nucleation of lithium disilicate glass. *J. Non-Cryst. Solids* **34**, 137–147 (1979).
8. L. Gránásy, P. F. James, Non-classical theory of crystal nucleation: Application to oxide glasses: Review. *J. Non-Cryst. Solids* **253**, 210–230 (1999).
9. R. P. Sear, Nucleation: Theory and applications to protein solutions and colloidal suspensions. *J. Phys. Condens. Matter* **19**, 033101 (2007).
10. U. Gasser, Crystallization in three- and two-dimensional colloidal suspensions. *J. Phys. Condens. Matter* **21**, 203101 (2009).
11. V. M. Fokin, E. D. Zanotto, Crystal nucleation in silicate glasses: The temperature and size dependence of crystal/liquid surface energy. *J. Non-Crystal Solids* **265**, 105–112 (2000).
12. H. Tanaka, Bond orientational order in liquids: Towards a unified description of water-like anomalies, liquid-liquid transition, glass transition, and crystallization. *Eur. Phys. J. E* **35**, 113–196 (2012).
13. M. Ediger, P. Harrowell, L. Yu, Crystal growth kinetics exhibit a fragility-dependent decoupling from viscosity. *J. Chem. Phys.* **128**, 034709 (2008).
14. E. D. Zanotto, D. R. Cassar, The race within supercooled liquids—Relaxation versus crystallization. *J. Chem. Phys.* **149**, 024503 (2018).
15. M. C. Weinberg, W. H. Poisl, L. Gránásy, Crystal growth and classical nucleation theory. *C. R. Chimie* **5**, 765–771 (2002).
16. T. Kawasaki, H. Tanaka, Formation of a crystal nucleus from liquid. *Proc. Natl. Acad. Sci. U.S.A.* **107**, 14036–14041 (2010).
17. J. Russo, H. Tanaka, The microscopic pathway to crystallization in supercooled liquids. *Sci. Rep.* **2**, 505 (2012).
18. J. Russo, H. Tanaka, Crystal nucleation as the ordering of multiple order parameters. *J. Chem. Phys.* **145**, 211801 (2016).
19. J. Russo, F. Romano, H. Tanaka, Glass forming ability in systems with competing orderings. *Phys. Rev. X* **8**, 021040 (2018).

20. P. Tan, N. Xu, L. Xu, Visualizing kinetic pathways of homogeneous nucleation in colloidal crystallization. *Nat. Phys.* **10**, 73–79 (2014).
21. H. Tanaka, T. Nishi, New types of phase separation behavior during the crystallization process in polymer blends with phase diagram. *Phys. Rev. Lett.* **55**, 1102–1105 (1985).
22. P. R. ten Wolde, D. Frenkel, Enhancement of protein crystal nucleation by critical density fluctuations. *Science* ***277***, 1975–1978 (1997).
23. V. Talanquer, D. W. Oxtoby, Crystal nucleation in the presence of a metastable critical point. *J. Chem. Phys.* ***109***, 223–227 (1998).
24. R. P. Sear, Homogeneous nucleation of a noncritical phase near a continuous phase transition. *Phys. Rev. E* **63**, 066105 (2001).
25. A. Shiryayev, J. D. Gunton, Crystal nucleation for a model of globular proteins. *J. Chem. Phys.* **120**, 8318–8326 (2004).
26. O. Galkin, G. Vekilov, Control of protein crystal nucleation around the metastable liquid–liquid phase boundary. *Proc. Natl. Acad. Sci. U.S.A.* **97**, 6277–6281 (2000).
27. O. Galkin, G. Vekilov, Nucleation of protein crystals: Critical nuclei, phase behavior, and control pathways. *J. Cryst. Growth* **1-4**, 63–76 (2001).
28. R. M. L. Evans, W. C. K. Poon, M. E. Cates, Role of metastable states in phase ordering dynamics. *Europhys. Lett.* **38**, 595–600 (1997).
29. S. K. Deb, M. Wilding, M. Somayazulu, P. F. McMillan, Pressure-induced amorphization and an amorphous-amorphous transition in densified porous silicon. *Nature* **414**, 528–530 (2001).
30. C. A. Angell, Formation of glasses from liquids and biopolymers. *Science* **267**, 1924–1935 (1995).
31. P. H. Poole, T. Grande, C. A. Angell, P. F. McMillan Polymorphic phase transitions in liquids and glasses. *Science* **275**, 322–323 (1997).
32. Y. Katayama, T. Mizutani, W. Utsumi, O. Shimomura, M. Yamakata, A first-order liquid-liquid transition in phosphorus. *Nature* **403**, 170–173 (2000).
33. W. Brazhkin, A. G. Lyapin, High-pressure phase transformations in liquids and amorphous solids. *J. Phys. Condens. Matter* **15**, 6059–6084 (2003).
34. O. Mishima, H. E. Stanley, The relationship between liquid, supercooled and glassy water. *Nature* **396**, 329–335 (1998).
35. J. C. Palmer, P. H. Poole, F. Sciortino, P. G. Debenedetti, Advances in computational studies of the liquid–liquid transition in water and water-like models. *Chem. Rev.* **118**, 9129–9151 (2018).
36. R. Kurita, H. Tanaka, Critical-like phenomena associated with liquid-liquid transition in a molecular liquid. *Science* **306**, 845–848 (2004)
37. H. Tanaka, General view of a liquid-liquid phase transition. *Phys. Rev. E* **62**, 6968–6976 (2000).
38. H. Tanaka, R. Kurita, H. Mataki, Liquid-liquid transition in the molecular liquid triphenyl phosphite. *Phys. Rev. Lett.* **92**, 025701 (2004).
39. M. Kobayashi, H. Tanaka, The reversibility and first-order nature of liquid–liquid transition in a molecular liquid. *Nat. Commun.* **7**, 13438 (2016).
40. K. Murata, H. Tanaka, Microscopic identification of the order parameter governing liquid–liquid transition in a molecular liquid. *Proc. Natl. Acad. Sci. U.S.A.* **112**, 5956–5961 (2015).
41. R. Kurita, H. Tanaka, Control of the liquid-liquid transition in a molecular liquid by spatial confinement. *Phys. Rev. Lett.* **98**, 235701 (2007).
42. K. Murata, H. Tanaka, Surface-wetting effects on the liquid-liquid transition of a single-component molecular liquid. *Nat. Commun.* **1**, 16 (2010).
43. K. Murata, H. Tanaka, Link between molecular mobility and order parameter during liquid–liquid transition of a molecular liquid. *Proc. Natl. Acad. Sci. U.S.A.* **116**, 7176–7185 (2019).
44. C. Huang *et al.*, Crystal nucleation rates in glass-forming molecular liquids: D-sorbitol, d-arabitol, d-xylitol, and glycerol. *J. Chem. Phys.* **149**, 054503 (2018).
45. S. Yip, Nanocrystals: The strongest size. *Nature* **391**, 532–533 (1998).
46. M. D. Uchic, D. M. Dimiduk, J. N. Florando, W. D. Nix, Sample dimensions influence strength and crystal plasticity. *Science* **305**, 986–989 (2004).
47. H. W. Sheng *et al.*, Polyamorphismin ametallic glass. *Nat. Mater.* **6**, 192–197 (2007).
48. M. H. Bhat *et al.*, Vitrification of a monoatomic metalic liquid. *Nature* **448**, 787–790 (2007).
49. C. A. Angell, Glass-formers and viscous liquid slowdown since David Turnbull: Enduring puzzles and new twists. *MRS Bull.* **33**, 544–555 (2008).